

# Preparation of silica-based hybrid materials coated on polypropylene film

SANG-YUP LEE\*, JAE-DONG LEE†, SEUNG-MAN YANG

*Department of Chemical Engineering, Korea Advanced Institute of Science and Technology, Taejon 305-701, Korea*

*E-mail: smyang@cais.kaist.ac.kr*

In this study, silica-based organic–inorganic hybrid coating materials were prepared by the sol–gel method. Tertaethoxysilane and polyvinyl alcohol were used as the inorganic and organic compounds, respectively. The substrate polypropylene film surface was modified by corona-plasma treatment to provide appropriate adhesion between the coating material and the polymer base film. A silane-coupling agent of vinyltriethoxysilane was also used to improve the adhesion between the base film and the coated layer. The effects of vinyltriethoxysilane in the hybrid materials were investigated using Fourier transform infrared analyses and X-ray diffraction. The vinyl group of vinyltriethoxysilane increased the hydrophobicity of the hybrid materials. The polypropylene films coated with the hybrid materials were characterized by examining their morphology, optical transparency and oxygen permeability. The results showed that the formation of hydrogen bonds between polyvinyl alcohol and the other compounds affected the microstructure of the coating solution and the final oxygen permeation property. Further, although the presence of vinyltriethoxysilane in the hybrid coating solution could improve adhesion between the coated layer and the polymer base film, it deteriorates the effectiveness of the barrier to prevent of oxygen permeation through the coated film. However, the coated film maintained visible transparency and even enhanced the transmission of long wavelength visible-light owing to refractive index matching. © 1999 Kluwer Academic Publishers

## 1. Introduction

The sol–gel method has been applied for the preparation of inorganic amorphous solids. By the use of highly reactive precursors, the sol–gel process has some advantages of practical significance including low temperature reaction and the ability to control the final composition with ease. Another merit of the sol–gel method is its convenience for the formation of various shapes, such as solid particle dispersion, monoliths, fibres and thin films, since sol–gel reaction proceeds through the phase transition from a liquid sol to a solid gel state [1, 2]. Furthermore, the sol–gel method also provides an easy way to produce a composite material. Simple mixing of the inorganic precursor and the organic compounds readily yields organic–inorganic hybrid materials. The organic functional groups incorporated into the inorganic silicate structure are the so-called organically modified ceramics (ORMOCER) or organically modified silicates (ORMOSIL) [3]. The ORMOCER exhibited intermediate properties between organic and inorganic materials.

Much interesting work has been done on organic–inorganic hybrid materials to determine their properties

[4–8]. An ORMOSIL that possessed both rubbery mechanical strength and glassy optical transparency was prepared successfully [4, 5]. One practically important application is the coating of an ORMOSIL solution onto a polymer film. Polymer films coated with organic–inorganic hybrid materials prepared with ORMOSIL showed an improved surface hardness in the Vickers hardness test [6]. In addition, hybrid materials forming a thin coated layer on polymer films cut down both oxygen and water vapour permeabilities [7, 8]. Most of these works have been done using polyethylene terephthalate (PET) or Nylon-6 as the substrate polymer film, since these polymer molecules with polar functional groups are, in themselves, compatible with the polar coating solutions.

However, these polymer films are too expensive to use as commercial packaging film, so that it is necessary to replace these with rather low-cost substrate films such as polypropylene (PP) or polyethylene (PE). Meanwhile, these polyolefin films have a drawback arising from their “non-polar” hydrophobic nature, which gives rise to a troublesome problem in enhancing adhesion between the coating layer and the substrate

\* Present address: Korea Institute of Science and Technology, Seoul 136-791, Korea.

† Present address: Samsung Electronics Co., Suwon 442-742, Korea.

film. To overcome this problem, two types of resolution strategies have been proposed:

1. Pretreatment of the polymer film surface either by plasma or primer treatment. Plasma treatment is now widely used in the manufacture of an inorganic material deposited film [9]. On the other hand, primer treatment is not so popular for it needs another coating step.

2. The other strategy is to employ a silane-coupling agent in the coating material to enhance the affinity between the inorganic material and the organic polymer material. The silicate compounds substituted by the organic functional groups are called the silane-coupling agent and this has been used widely in dye, adhesive, paint and so on. In fact, the silane-coupling agent is a kind of ORMOSIL in itself. It is well known that the organic functional group enhances the adhesion between the polar and non-polar layers [6]. However, few efforts have been made to determine the overall properties of the hybrid materials with the silane-coupling agent, and their effects on the final properties of polymer films coated with hybrid materials have not been fully understood yet.

In the present work, an ORMOSIL coating solution with a silane-coupling agent was prepared through the sol-gel method and layered on the PP film by spin coating. The polyolefin PP film was pretreated with corona-plasma to enhance phase adhesion. The pretreated PP film surface was characterized by various methods, such as contact angle measurement and X-ray photoelectron spectroscopy (XPS). Vinyltriethoxysilane (VTES) was used as a silane-coupling agent and tetraethoxysilane (TEOS) and polyvinyl alcohol (PVA) were used as an inorganic precursor and an organic compound, respectively. These substances were mixed together and underwent sol-gel reaction. After the organic-inorganic hybrid sol solution was coated on the pretreated PP film, gelation and drying followed subsequently. To investigate characteristics of the hybrid materials prepared here, the coating solutions were characterized by Fourier transform infrared (FTIR) analysis and X-ray diffraction (XRD). The solid phase morphology in the sol solution was observed through transmission electron microscopy (TEM) before spin coating. The coated film surface and cross-sectional images were observed through scanning electron microscopy (SEM) and its pore size was measured through nitrogen adsorption with Brunauer-Emmett-Teller (BET) apparatus. Finally, the oxygen permeability and the optical transparency as final properties of the coated film were measured to examine the effects of VTES addition in the hybrid materials.

## 2. Experimental procedure

A commercial grade PP film (Honam Petrochemical Co.) was used as the substrate. The film was prepared by two consecutive steps. First, pellets of the base resin were melted at 230 °C. Then, the film was drawn at a speed of 10 m min<sup>-1</sup> to an average thickness of about 70 μm and a width of 29 cm. During the drawing pro-

cess, the surface of the PP film was treated simultaneously by corona plasma with an electronic energy of 60 V and 4 A at atmospheric temperature. Thus, the total treatment energy consumed per unit length of substrate film was 24 W min<sup>-1</sup> m<sup>-1</sup>.

The organic-inorganic hybrid coating solution was prepared as follow: TEOS (Aldrich, 98%) and VTES (Shin Etsu Silicone Co.) were mixed in ethanol (EtOH; GR grade, Merck) with various molar ratios. The mixture was stirred with a magnetic stirrer for 3 min to ensure a homogenized state. Then, 3.6 ml of acidic water at pH 0.28 was added to the mixture to proceed the sol-gel reaction. Hydrochloric acid (HCl, Junsei Chem.) was added into deionized water to control the pH of the acidic water. The molar ratio of EtOH to the TEOS-VTES mixture and that of water to the TEOS-VTES mixture was maintained at 1 and 2, respectively. After mixing the solution for 30 min, PVA (Aldrich: 80% hydrolysed; average *M<sub>w</sub>* 9000-10 000) and distilled water were added to produce a hybrid coating solution. The volume of the added water was 18 ml and a different amount of PVA was added to each coating solution. The various compositions of the prepared coating solutions are contained in Table I. For convenience, the coating solutions in Table I were classified with labels; the coating solutions made of the binary mixture of TEOS-VTES without PVA were denoted by the prefix TV, and those of the ternary mixture of TEOS-VTES-PVA were denoted by the prefix TVP. The numbers next to the prefix represented the composition of the constituent substances. For example, the sample of TVP485 in Table I denoted a hybrid material prepared from 0.04 mol of TEOS, 0.08 mol of VTES and 5 g of PVA. The solution was mixed again for 90 min and then coated on the substrate film. Then, the coated film was dried at 100 °C for 8-14 min in a drying oven. Finally, the dried film was kept in a petri dish at room temperature.

TABLE I Compositions of TEOS, VTES and PVA for the hybrid coating materials

	TEOS (mol)	VTES (mol)	PVA (g)
VTES	0.00	0.10	0.0
TV19	0.01	0.09	0.0
TV28	0.02	0.08	0.0
TV37	0.03	0.07	0.0
TV46	0.04	0.06	0.0
TV64	0.06	0.04	0.0
TV82	0.08	0.02	0.0
TEOS	0.10	0.00	0.0
TVP002	0.00	0.00	2.5
TVP005	0.02	0.00	5.0
TVP405	0.04	0.00	5.0
TVP805	0.08	0.00	5.0
TVP025	0.00	0.02	5.0
TVP045	0.00	0.04	5.0
TVP085	0.00	0.08	5.0
TVP145	0.01	0.04	5.0
TVP245	0.02	0.04	5.0
TVP445	0.04	0.04	5.0
TVP485	0.04	0.08	5.0
TVP4125	0.04	0.12	5.0
TVP442	0.04	0.04	2.5
TVP446	0.04	0.04	6.5

The substrate PP film was characterized by measuring the contact angle against distilled water and diiodomethane ( $\text{CH}_2\text{I}_2$ ), as proposed by Wu [10]. The contact angle measurement was performed seven times through a microscope with a protractor eyepiece at room temperature and the average value was taken. From the contact angles, the polar and the dispersion surface tensions, and the surface polarity were calculated. Oxygen and carbon peaks in the XPS spectra were also detected on the PP film before and after pretreatment to confirm the effect of corona-plasma treatment.

The coating solution was gelled and dried at room temperature over two weeks and characterized by various methods, such as FTIR spectroscopy, XRD and water vapour absorption testing. The dried gel of the coating solution was pulverized, mixed with KBr and pelletized for infrared (i.r.) spectroscopy. Scanning was performed ten times in the range  $400\text{--}4000\text{ cm}^{-1}$ . The i.r. spectrogram was calibrated by setting up the base line correction. In order to test water vapour absorption by the dried coating solution, the pulverized gels were dried at  $60\text{ }^\circ\text{C}$  in a vacuum drying oven for 24 h and placed in a vessel at a relative humidity corresponding to a saturation value at  $55\text{ }^\circ\text{C}$ . The weight increment of the dried gel was measured with elapsed time. XRD was taken over the range of  $2\theta = 2\text{--}70^\circ$  at a condition of 40 V and 45 mA to investigate the effects of TEOS and VTES on the crystal growth of PVA. The pore sizes with various VTES contents were determined through  $\text{N}_2$  adsorption isotherms measured by BET (ASAP2010). The surface and the cross-sectional morphologies of the coated film were observed through an SEM (535M, Philips). In observing the SEM images, the samples were slanted  $30^\circ$  to view the surface morphology clearly. The oxygen permeability of the coated film was measured at room temperature by a commercial gas transmission rate tester (M-C3, Toyo Seiki Seisaku-Sho Co.), which complied with ASTM (D-1434-75M). Oxygen permeability was calculated by the measured gas transmission rate based on the high vacuum time-lag technique, as proposed by Barrer [11]. Finally, the light transparency of the coated film was examined by the transmission ratio measurement in the visible-light wavelength range of  $250\text{--}850\text{ nm}$  with an ultraviolet–visual (u.v.–vis.) spectrometer.

### 3. Results and discussion

#### 3.1. Characterization of substrate film and hybrid coating material

To improve adhesion with the hybrid coating material, the base film of PP was pretreated with corona-plasma at a treatment energy of  $24\text{ W min}^{-1}\text{ m}^{-1}$ . The XPS result confirmed that corona-plasma treatment created on the PP film polar surface functional groups, such as carbonyl and carboxyl groups, and nitrogen oxide compounds on the PP film [12]. To check the changes in surface polarity of the pretreated PP film, the contact angles versus water and diiodomethane ( $\text{CH}_2\text{I}_2$ ) were measured and shown to be  $62.0$  and  $44.9^\circ$ , respectively. The dispersion and the polar surface tensions were de-

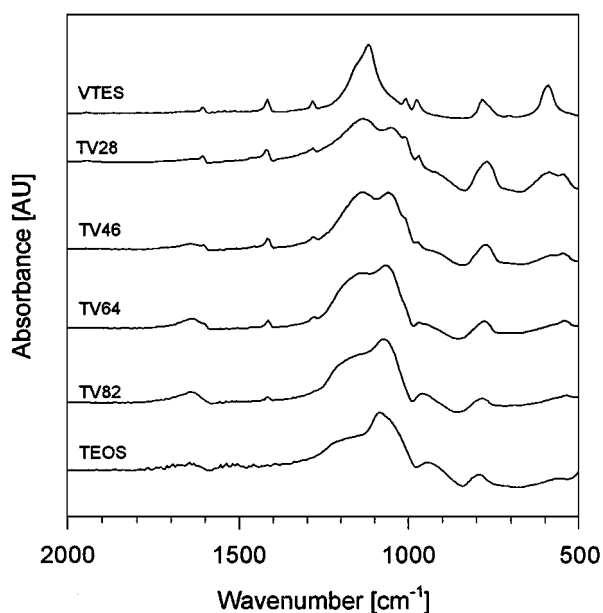


Figure 1 I.r. spectra of the binary hybrid gels TEOS–VTES with various compositions.

termined to be  $26.724$  and  $20.599\text{ mN m}^{-1}$ , respectively. Thus, the polarity of the pretreated substrate film was  $0.435$ , which was large compared with  $0.167$  for the untreated PP film. It is obvious from the present results that although corona pretreatment enhanced the surface polarity, considerable amounts of the surface functional groups still remained non-polar. Therefore, corona-plasma pretreatment alone was not sufficient to create a proper surface polarity on the virgin PP film, which was required for satisfactory adhesion with the polar coating solution. Thus, the silane-coupling agent VTES was added in the preparation of the sol–gel process to enhance adhesion between the coated layer and the non-polar functional groups on the PP film surface.

FTIR spectrograms of the pulverized and dried samples of TEOS–VTES hybrid gels with various molar ratios are shown in Fig. 1. The pure TEOS and VTES samples have typical peaks at  $1060$  and  $1140\text{ cm}^{-1}$ , respectively. It is also noteworthy that the VTES content increases from 0 to 100 from  $1060$  to  $1140\text{ cm}^{-1}$ , which is characteristic of the silicate oxide (Si–O–Si). In the intermediate compositions of TEOS–VTES, these characteristic peaks were slightly broadened due to chemical bonds between the constituent molecules. A hybrid of these two compounds was also reported by Iwamoto and Mackenzie [6]. In addition, typical vinyl group peaks were detected at  $584$ ,  $968$  and  $1604\text{ cm}^{-1}$ . These are due to the fact that after gelation the vinyl groups still remained unconverted without experiencing any chemical reaction. The remaining vinyl groups influenced the junction of the network and induced hydrophobicity in the coating layer [13, 14]. The peaks at  $1640\text{ cm}^{-1}$ , which appeared from the pure TEOS to the sample TV46, are indicative of the fact that water absorption by the silicate oxide occurred for the samples with a VTES content less than 60 mol %. Thus, the FTIR spectra clearly imply that the increment of VTES content improved the hydrophobicity of the coating layer.

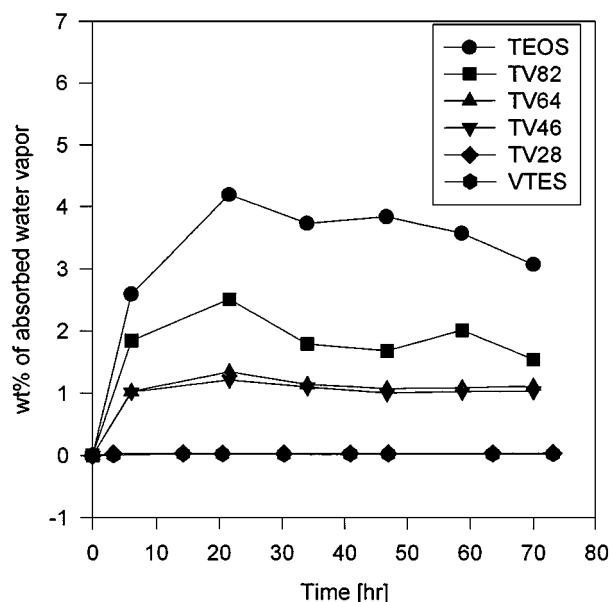


Figure 2 Relative weight of the adsorbed water in the binary gel TEOS–VTES with various compositions. The relative weight was scaled with respect to the weight of dried gel.

The enhanced hydrophobicity can be deduced by measuring the weight of the absorbed water vapour. In Fig. 2, the weight per cent of the absorbed water vapour relative to the weight of the dried sample was plotted as a function of time for various VTES contents. Indeed, water absorption was prohibited considerably by the presence of the hydrophobic vinyl groups of VTES. The weight per cent of the absorbed water vapour at the saturated state was about 4 wt % for pure TEOS and gradually decreased as the VTES content increased. In particular, the saturated water absorption for the sample with 80 mol % VTES was as low as 0.025 wt % for the pure VTES sample. Thus, the silane-coupling agent VTES can be used as a waterproof substance, which has a barrier property against water vapour, as reported by Zhang *et al.* [15].

Although the addition of VTES enhanced both the adhesion and the resistance to water vapour, coated solutions with high VTES contents exhibited phase separation between solid and liquid in the sol. In this case, a non-uniform coating solution was obtained inevitably. In this study, PVA was added not only to overcome the non-uniformity of the hybrid coating material but to improve the oxygen barrier property. In the sol–gel reaction in the presence of PVA, the hydrophobicity induced by VTES would affect the chemical connection between PVA and TEOS–VTES sol. The i.r. spectra of TEOS–VTES–PVA samples for various compositions are shown in Fig. 3. As noted, the increment of TEOS content (or equivalently the enhanced hydrophilicity) reduced the relative intensity of the peak at around 2800–3000  $\text{cm}^{-1}$ , which was typical of PVA. In general, a hydrogen bond is formed between the silicate oxide surface and the hydroxyl groups of PVA [16]. Thus, it can be inferred from the i.r. spectra that a chemical reaction or formation of a hydrogen bond occurred between TEOS and PVA.

Let us now consider the phase uniformity and morphology of the coating. It is worthy of note that the exist-

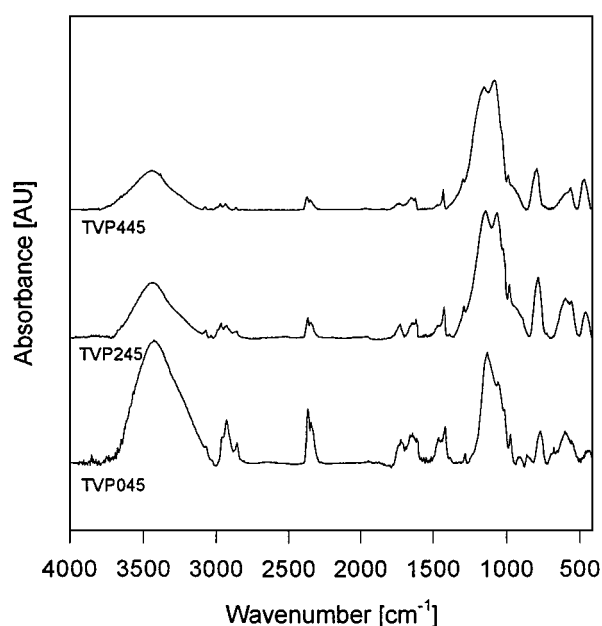


Figure 3 I.r. spectra of the ternary hybrid gels TEOS–VTES–PVA with various TEOS contents.

tence of the vinyl groups of VTES lessens the probability of hydrogen bond formation between the hydrolysed inorganic compounds and the PVA molecules owing to their intrinsic hydrophobicity. Thus, it is expected that the presence of VTES molecules will cause morphological changes and an alteration in the overall performance of the coated film. In Fig. 4, TEM images of the coating solutions are reproduced for various compositions. The samples were prepared by dilution of the coating solution with ethanol. As seen clearly from Fig. 4a for the TEOS–VTES sample, solid phases in the sol grew irregularly and phase separation occurred between the VTES solid particles and the liquid phase. The non-uniformity in the binary system of TEOS–VTES became pronounced with time. In this case, the films were coated irregularly and were opaque with poor light transparency, as we shall see shortly. Meanwhile, the binary coating solution of TEOS–PVA in the absence of VTES was homogeneous and exhibited a well distributed networked structure in the sol solution, as shown in Fig. 4b. For the VTES–PVA binary system, the structure of the coating solution looks like an intermediate state between the binary systems of TEOS–VTES and TEOS–PVA. As noted from Fig. 4c, although the binary system of VTES–PVA possessed a networked structure, the uniformity of the coating solution was not so good as the TEOS–PVA solution. It can be readily seen from Fig. 4d that the addition of PVA in the TEOS–VTES sol created a relatively uniform structure of solid phases compared with the TEOS–VTES sol solution. However, the ternary system TEOS–VTES–PVA did not exhibit phase structure so good as the binary system of TEOS–PVA. It is thus obvious that the addition of VTES molecules inhibited homogeneous phase–structure formation between the inorganic silicate phase network and PVA. This is because the VTES molecules diminished the conjunction between the inorganic network and the hydroxyl groups

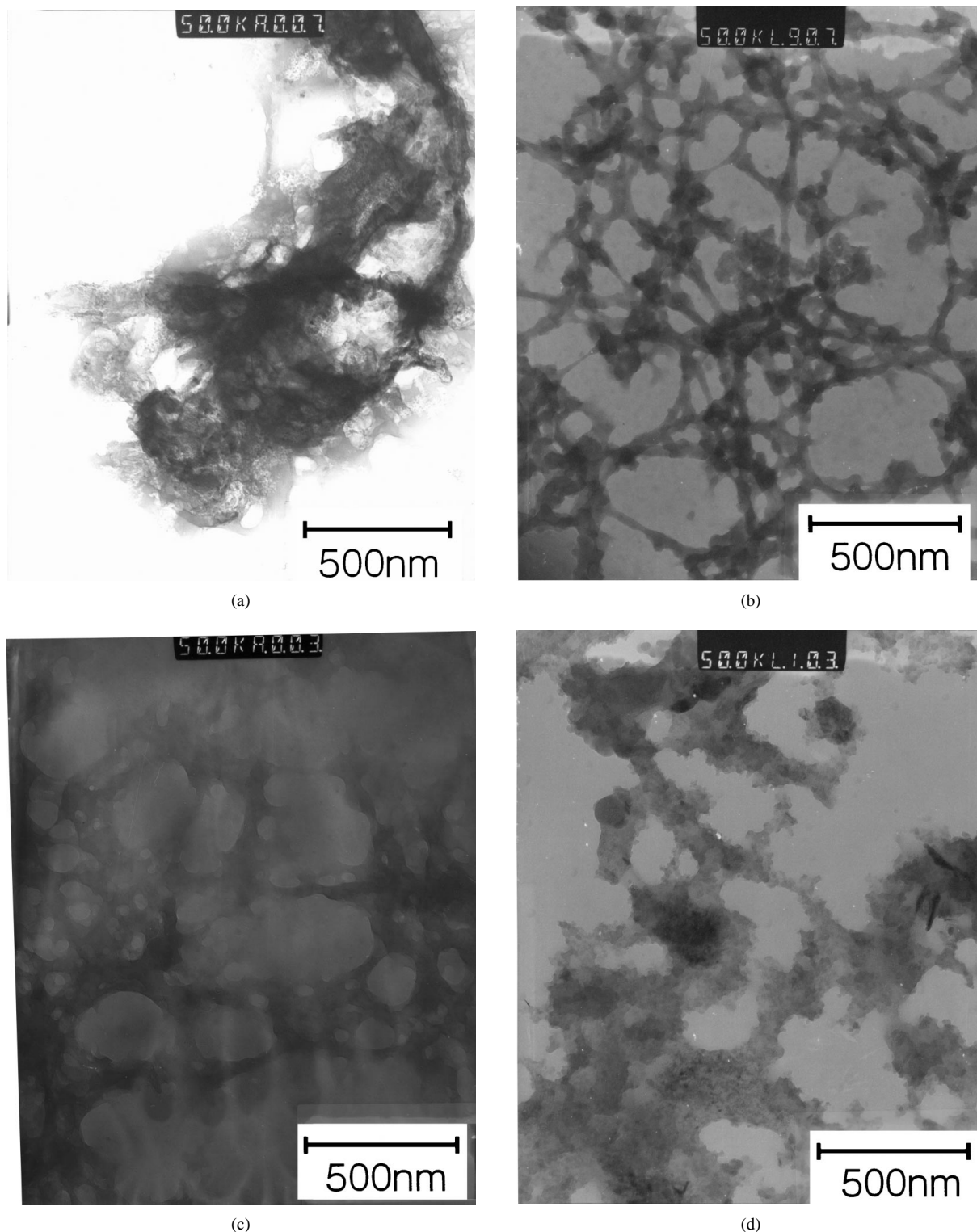


Figure 4 TEM images of the coating solutions at sol state for various compositions. (a) TV28, (b) TVP205, (c) TVP025, and (d) TVP145.

of PVA or prevented the PVA molecules from filling the inorganic gel pores.

X-ray diffractograms of the hybrid materials contained in Fig. 5 provided clear evidence for the effect of the VTES molecules on the crystallinity of PVA. As expected, a sharp characteristic peak appears at  $2\theta = 19^\circ$  for pure PVA. The addition of TEOS into pure PVA broadens the PVA peak. This implies that TEOS retarded the crystal growth of PVA by the formation of a hydrogen bond or by reaction between these two components [17]. On the other hand, the presence of VTES

in the PVA phase induced only little changes in the crystal growth of PVA. As seen from Fig. 5, the PVA peak in the VTES–PVA binary system was as sharp as that of pure PVA, since the hydrogen bond or chemical reaction between VTES and PVA was negligible.

Since a hydrogen bond plays the most important role in forming the connection between the inorganic sol and the organic PVA, there is little possibility of a proper association between the inorganic VTES sol and PVA. Thus, it is obvious that phase separation or a segregated microdomain could be formed in the binary VTES and

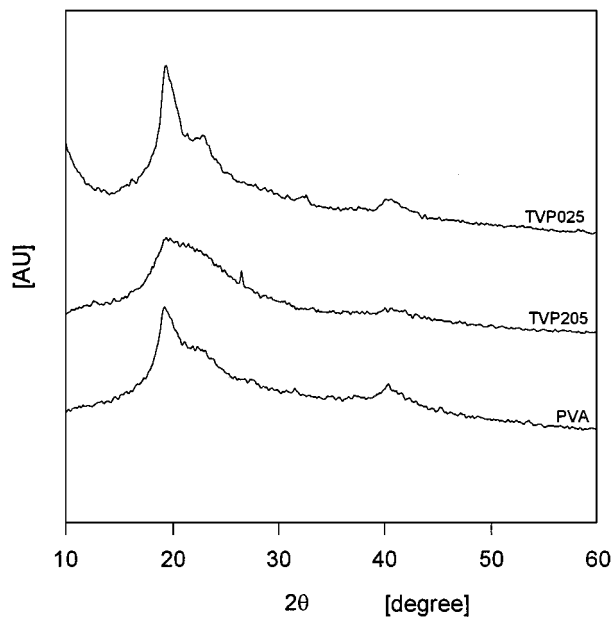


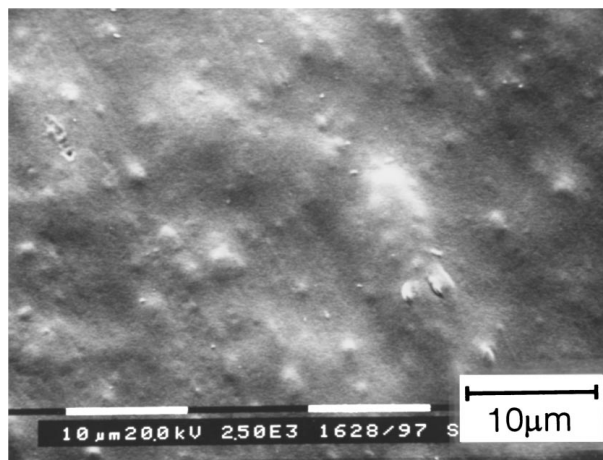
Figure 5 Changes in the XRD pattern by the addition of TEOS or VTES to PVA.

PVA system. Consequently, VTES molecules could not interrupt effectively the crystal growth of PVA, as confirmed by XRD.

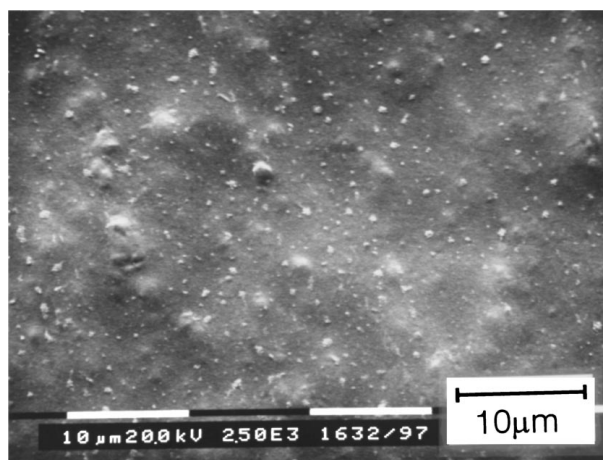
### 3.2. Properties of the coated PP film

Coated film morphologies were observed with an SEM and their microphotographs for various compositions were consistent with the results obtained from TEM and XRD analyses for the hybrid coating solutions. The SEM microphotographs for various compositions are shown in Figs 6 and 7. The average thickness of the coated layer is about  $1.3 \mu\text{m}$  for the binary TEOS–VTES system. It can be seen from Fig. 6a that the film coated with VTES alone possessed somewhat polymeric surface morphology. However, as the TEOS content increased in the binary TEOS–VTES system, the coated film surface exhibited a glassy morphology. When the TEOS content was above 30 mol %, the coated films underwent severe cracking in the drying process, as shown in Fig. 6c. In Fig. 7, SEM microphotographs of the binary system VTES–PVA are reproduced. The average film thickness of the VTES–PVA system was about  $3 \mu\text{m}$ . Also included in Fig. 7a is an SEM image of the film coated with PVA alone. The PVA coated film showed smooth surface morphology. Although the addition of VTES made the surface morphology rough, film adhesion between the coated layer and the PP base film was satisfactory.

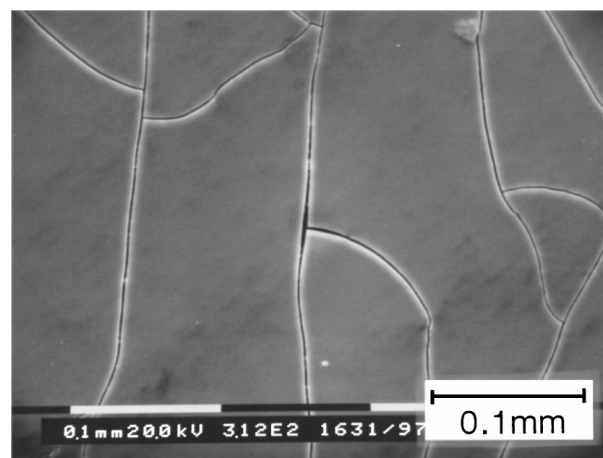
Let us now consider the effect of the coated layer on the oxygen permeability of the PP film. In the present study, the permeability was measured at room temperature. In Fig. 8, the oxygen permeability of the PP film coated with the TEOS–VTES hybrid solution is illustrated as a function of VTES content. The TEOS–VTES layer coated on the PP film made little effect on oxygen permeation, considering that the oxygen permeability of the bare PP film was about  $1.5 \times 10^{-10} \text{ cm}^3 \text{ cm cm}^{-2} \text{ s}^{-1} \text{ mmHg}^{-1}$ . Meanwhile, the pure VTES layer



(a)



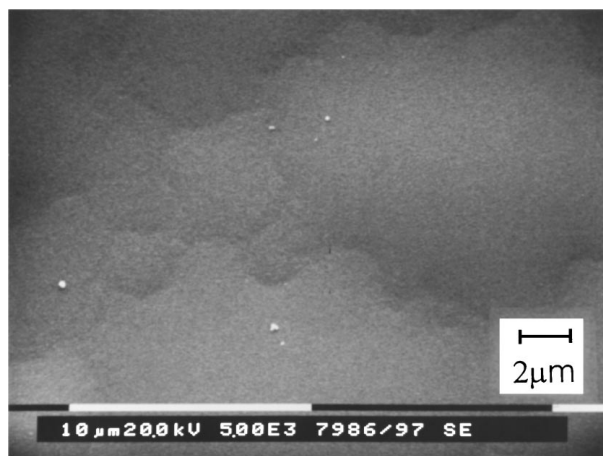
(b)



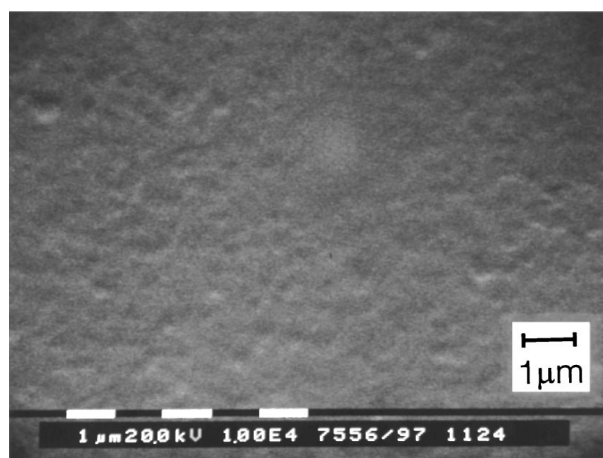
(c)

Figure 6 SEM images of film surfaces coated with the binary hybrid gel TEOS–VTES: (a) VTES, (b) TV28, and (c) TV55.

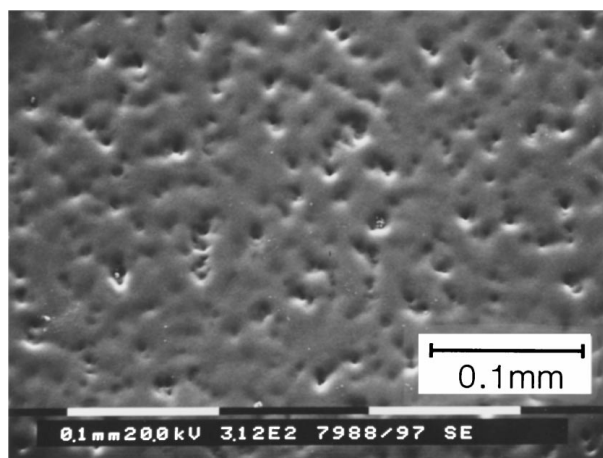
cut the oxygen permeability by about 30% from that of the bare PP film. These results were due to the formation of micropores on the coated layer of TEOS–VTES. As mentioned earlier, the vinyl groups of VTES in the binary system of TEOS–VTES played a role as a network modifier and interrupted the formation of a dense silicate network structure. In Fig. 9, the pore radius of the TEOS–VTES layer coated on the PP film was plotted versus VTES content. Indeed, the changes in pore radius of the TEOS–VTES layer were consistent with the



(a)



(b)



(c)

Figure 7 SEM images of film surfaces coated with the binary hybrid gel VTES–PVA: (a) PVA, (b) TVP045, and (c) TVP085.

oxygen permeability variations in Fig. 8. Thus, larger pores were formed for higher VTES content. However, the pore radius was smallest for the pure VTES layer, which also agreed well with the permeability data.

Gas flow through a narrow channel is usually attributed to ordinary bulk diffusion, pressure driven viscous flow and so-called Knudsen diffusion. However, when the mean free path of the permeating gas is much larger than the pore size, Knudsen flow is the predominant transport mechanism. Since the mean free path of oxygen at 25 °C is about 73 nm and the pore radius

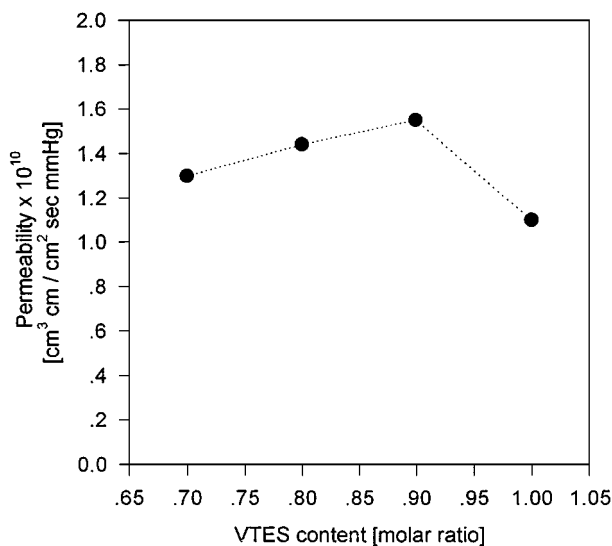


Figure 8 Oxygen permeability of the coated film as a function of VTES molar ratio in the binary coating solution TEOS–VTES.

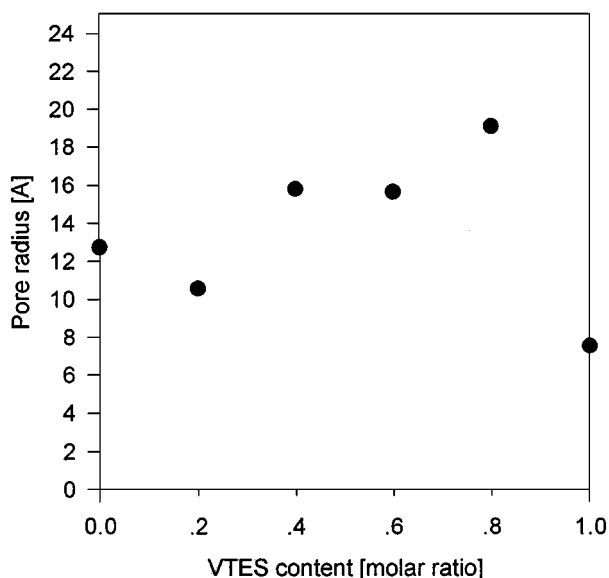


Figure 9 Average pore radius of the binary hybrid gel TEOS–VTES as a function of VTES molar ratio.

ranges from 0.8 nm to 1.8 nm, Knudsen flow is the dominant transport mechanism through the coated layer of TEOS–VTES. Although the pore radius for Knudsen flow is small enough to be predominant, the pore size of the coated layer of TEOS–VTES is too large to retard oxygen permeation. Thus, the organic component PVA was added to improve the oxygen barrier property.

In Fig. 10, oxygen permeability of the PP film coated with the ternary solution TEOS–VTES–PVA is illustrated as a function of TEOS content. The samples used in this plot contained 0.04 mol VTES and 5 g PVA, both of which were fixed. Also shown in Fig. 11 is oxygen permeability versus the PVA content for the coating solution with TEOS and VTES, each of 0.04 mol. As clearly seen from Figs 10 and 11, the increment in either TEOS or PVA content (or equivalently the reduction of VTES content in the ternary solution) gave rise to considerable reduction of oxygen permeation through the coated film. For illustrative purposes,

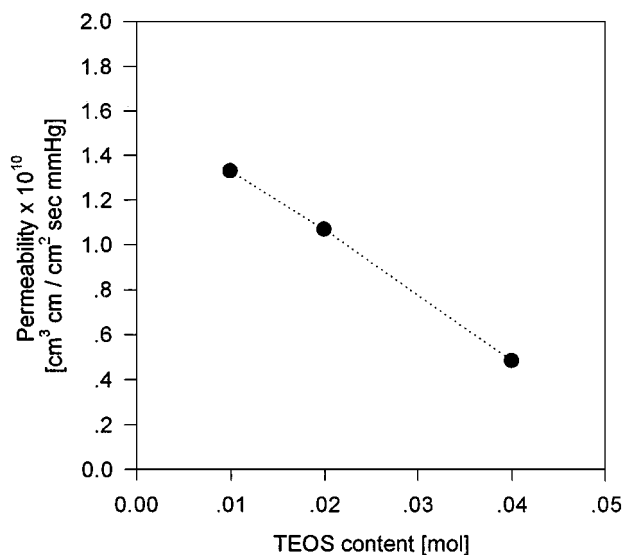


Figure 10 Oxygen permeability of the coated film as a function of TEOS content in the ternary coating solution TEOS–VTES–PVA. The samples contained 0.04 mol VTES and 5 g PVA.

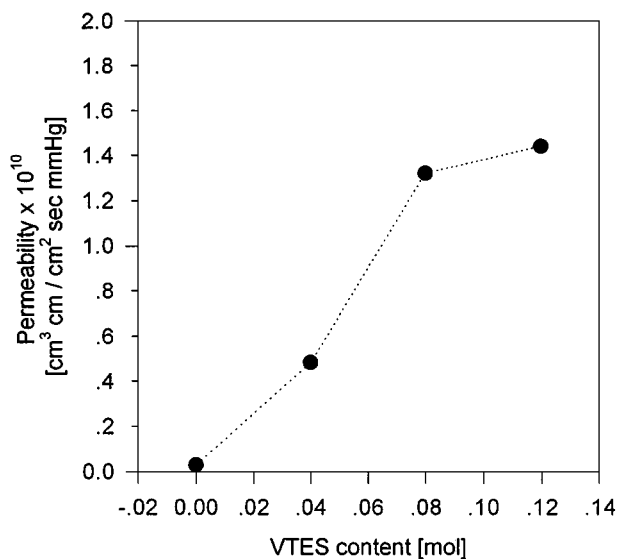


Figure 12 Oxygen permeability of the coated film as a function of VTES content in the ternary coating solution TEOS–VTES–PVA. The samples contained 0.04 mol TEOS and 5 g PVA.

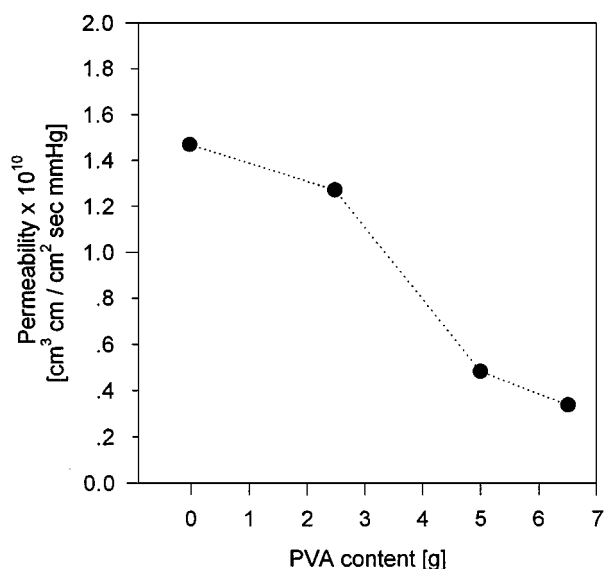


Figure 11 Oxygen permeability of the coated film as a function of PVA content in the ternary coating solution TEOS–VTES–PVA. The samples contained TEOS and VTES, each of 0.04 mol.

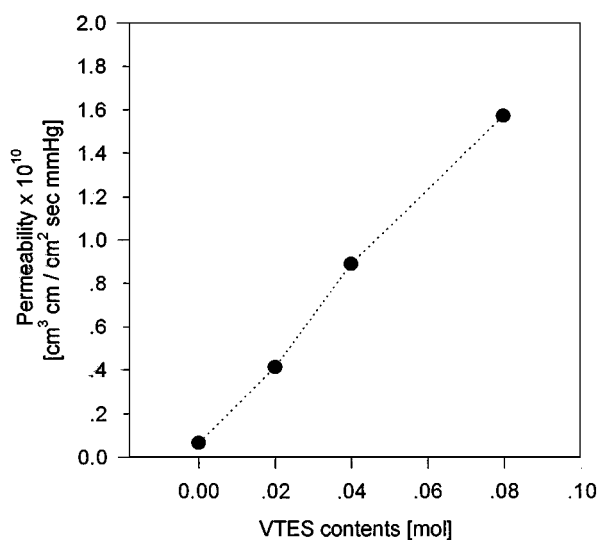


Figure 13 Oxygen permeability of the coated film as a function of VTES content in the binary coating solution VTES–PVA. The samples contained 5 g PVA.

oxygen permeability versus VTES content is shown in Fig. 12 for the coating solution with 0.04 mol TEOS and 5 g PVA. Indeed, the presence of VTES deteriorates the effectiveness of the barrier to prevent oxygen permeation. This can be readily expected from the behaviour of the phase structure of the coating solutions, as discussed previously in the sections on TEM and XRD analyses. The same trend was also preserved in the binary system VTES–PVA, as indicated in Fig. 13 in which oxygen permeability is plotted versus VTES content for a coating solution with 5 g PVA. Comparison of Figs 12 and 13 shows that the deteriorating effect of VTES is pronounced in the absence of TEOS. It can be deduced from the oxygen permeation results that the VTES molecules created micropores in the inorganic solid phase, and that their vinyl groups, which possessed strong hydrophobicity, prohibited the PVA molecules from filling the pores. Thus, although the

added VTES enhanced adhesion to the hydrophobic substrate film of PP, it increased oxygen permeation through the coated film.

Finally, let us turn to the effect of the coated layer on light transmission through the coated PP film. In Fig. 14, relative light transmission is illustrated as a function of light wavelength for various compositions of the hybrid coating solutions. As seen from the figure, light transmission through the film does not decrease and visual transparency of the film is maintained after coating. In the long visible wavelength limit, relative light transmission is even improved by the coated layer. On the other hand, light transmission is slightly reduced in the short visible wavelength limit. Transparency enhancement in the long visible wavelength region is due mainly to refractive index matching between the organic–inorganic hybrid coated layer and the PP base film. Meanwhile, reduced transmission in the short visible wavelength region is caused by small



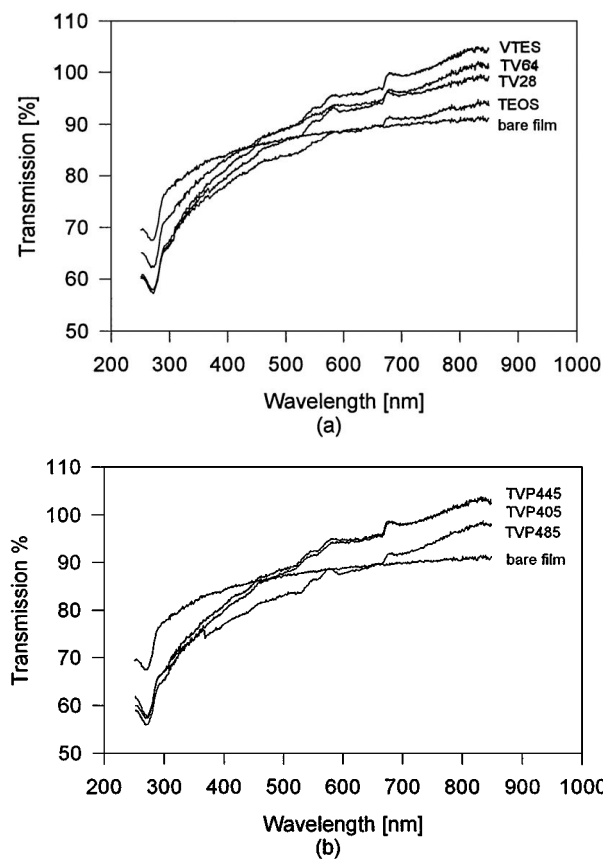


Figure 14 Light transmission through the coated film as a function of wavelength for various compositions: (a) TEOS-VTES solutions, and (b) TEOS-VTES-PVA solutions.

pores in the coated film. The small pores scatter the visible light and cut down visible-light transmission.

#### 4. Conclusions

Hybrid coating materials of TEOS-PVA were prepared by the sol-gel method and coated on PP base film. The silane-coupling agent VTES was added to enhance adhesion between the coated layer and the polymer base film. The effects of VTES addition on phase morphology and upon the characteristics of the coating solution were investigated using FTIR, XRD and TEM. The VTES vinyl groups improved the hydrophobicity of the hybrid materials and thereby enhanced both adhesion between two contiguous layers and resistance to water vapour absorption. The morphological behaviour observed through TEM for various VTES contents in the coating solution was consistent with the results ob-

tained from oxygen permeation through the coated film. The addition of VTES increased oxygen permeability, for its hydrophobic vinyl group retarded the formation of a dense structure between the inorganic silicate and the organic PVA phase. The oxygen permeability of the coated PP film was reduced considerably by the addition of VTES in the ternary system TEOS-VTES-PVA. Finally, transmission of long wavelength visible-light through the coated PP film was increased at the expense of the transmission of short wavelength visible-light, compared with the bare PP film.

#### Acknowledgements

This work was supported by the Korea Science and Engineering Foundation (KOSEF) under grant 971-1109-058-2. Honam Petrochemical Research Center kindly provided the PP base films and corona-plasma facility and the R&D Center of SK Corp. helped us to measure gas permeability. The authors appreciate their support.

#### References

1. H. DISLICH, *J. Non-Cryst. Solids* **73** (1985) 599.
2. D. R. ULRICH, *Chemtech*, **April** (1985) 242.
3. R. M. LAINE (ed.), in "Inorganic and Organometallic Polymers with Special Properties" (Kluwer Academic, Netherlands, 1992), 297.
4. Y. HU and J. D. MACKENZIE, *J. Mater. Sci.* **27** (1992) 4415.
5. A. B. WOJCIK and L. C. KLEIN, *Appl. Organometallic Chem.* **11** (1997) 129.
6. T. IWAMOTO and J. D. MACKENZIE, *J. Mater. Sci.* **30** (1995) 2566.
7. Y. TOSHIKI and M. RYUKICHI, *Jpn. Kokai Tokkyo Koho JP06* **192** (1994) 454.
8. K. TADANAGA, K. IWASHITA, T. MINAMI and N. TOHGE, *J. Sol-Gel Sci. Tech.* **6** (1996) 107.
9. LOHWASSER and WOLFGANG, Patentschrift (Switz.) CH 682 (1993), 821.
10. S. WU, *J. Polym. Sci.: Part C* **34** (1971) 19.
11. R. M. BARRER, *Trans. Faraday Soc.* **35** (1939) 628.
12. S. WU, in "Polymer Interface and Adhesion," 1<sup>st</sup> Edition, (Marcel Dekker, New York, 1982) p. 307.
13. K. TADANAGA, K. AZUTA and T. MINAMI, *J. Ceram. Soc. Jpn* **105** (1997) 555.
14. W. LI and R. J. WILLEY, *J. Non-Cryst. Solids* **212** (1997) 243.
15. Z. ZHANG, Y. TANIGAMI, R. TERAJ and H. WAKABAYASHI, *ibid.* **189** (1995) 212.
16. R. K. ILER, *J. Colloid Interface Sci.* **51** (1975) 388.
17. S. YANO, T. FURUKAWA, M. KODOMARI and K. KURITA, *Kobunshi Ronbunshu* **53** (1996) 218.

Received 1 June  
and accepted 26 August 1998